7th World Congress on Civil, Structural, and Environmental Engineering (CSEE'22)
~~Lisbon, Portugal~~ Virtual Conference – April 10 - 12, 2022
Paper No. ICSECT 109
DOI: 10.11159/icsect22.109

First Results of the Application of Infrared Thermography to the Crack Inspection in Wooden Beams

Miguel Gallego [1], Manuel Cabaleiro [1], Ivan Garrido [2], Borja Conde [1], Belen Riveiro [1,]
[1]Department of Materials Engineering, Applied Mechanics and Construction, University of Vigo,
C.P. 36208, Vigo, Spain
mgc995@gmail.com; mcabaleiro@uvigo.es; bconde@uvigo.es; belenriveiro@uvigo.es
[2]GeoTECH Group, CINTECX,
Universidade de Vigo, 36310 Vigo, Spain.
ivgarrido@uvigo.es

Abstract **-** Wooden structures are exposed to degradation during their lifetime. There are a large number of wooden structures around the world, some of them historical which are patrimony of humanity. Structural health inspection is a priority task to be applied to such structures in order to prevent or mitigate the effect of degradation, but nowadays this health inspection is generally manual. Therefore, the development of methodologies that allow to automate the structural health inspection is a goal of maximum priority. Among the most common defects that appear in wooden structures due to degradation are the cracks. Although the structural health inspection of wooden structures is generally manual, some methods have been applied for the automatic inspection of cracks using different techniques, such as laser scanner or photogrammetry. However, the estimation of crack depth is beyond the scope of these techniques. Moreover, InfraRed Thermography (IRT) has proved to be a useful tool for estimating the depth of different types of defects.Then, this work introduces IRT as a technique for the automatic inspection of superficial cracks in wooden beams. Specifically, the width, long and depth of the cracks are estimated through the development of two different methodologies: (i) the first method consists of the analysis of the thermal images acquired without previous thermal excitation on the wooden beams, and (ii) the second method consists of the analysis of the thermal image sequence acquired during the cooling after a thermal excitation in each wooden beam. The results of this work show that both methodologies can be used as a basis for the future automatization of crack inspection in wooden beams.

Keywords**:** Thermography, Crack, Inspection, Structural Health

1. Introduction

Wood is a common material used in different structures around the world, mainly in historical structures. For this reason, the use of methodologies that facilitate the structural health inspection in wooden structures is a very important goal.

Cracks in wood is one of the main effects of the degradation to this material. Most of the cracks are usually harmless, but the analysis of their sizes, depths, positions, and evolutions is a priority task during the structural health inspection of wooden structures. For the automatic inspection, there are some methodologies that use techniques without needing to make contact with the structures, such as laser scanner. This technique can be used for crack inspection in wood, such as it is shown in the paper of Cabaleiro et al. [1]. In that study, laser scanner data is used to identify the position and estimate the size of the crack in wooden beams by the proposed methodology, but without being able to estimate the depth. The laser scanner has been used in several works to control the structural health of wood [2] [3] [4] . Photogrammetry technique is also used in the automatic crack inspection in wooden beams but being not possible the measurement of depth [5].

InfraRed Thermography (IRT) is a promising technique that is increasingly used in Non-Destructive Testing (NDT). The IRT tests are performed without making contact with the material. Another advantage is that IRT does not damage the material if the technique is used correctly [6] [7] [8] [9] [10].

IRT measures the amount of infrared radiation that is emitted from the different parts of the surface of a body, converting the infrared radiation to temperature by the Stefan-Boltzmann law. Different amounts of infrared radiation are converted to different temperature values [5] [6] [7]. Thus, the identification and geometric and thermal characterisation of surface defects and internal defects (with a range of a few centimetres in deep) is possible due to their different thermophysical parameters with respect to their unaltered surroundings, defects such as: moisture, delamination, mould, infiltrations, cracks, etc.

Despite the advantages of IRT and the large number of published IRT papers on crack inspection [11] [12] [13] [14] [15] [16] [17], the geometric analysis of cracks in wood from thermal images has not been conveniently addressed on the current literature [17]. So, the objective of this work is to use IRT to identify and measure width, long and depth of superficial cracks in wood beams, allowing to establish the basics for the future automatization of crack inspection in wooden beams.

2. Material and test performed.

Two wooden beams are tested, which present the following characteristics: (i) one is a pine beam with dimensions 100x17.4x11.4 cm, and (ii) the second is an oak beam with dimensions 63x25x14.4 cm. These beams are disposed 2 meters away from the thermographic camera, being the direction of the camera's focus perpendicular to the surface analysed (see Figure 1).

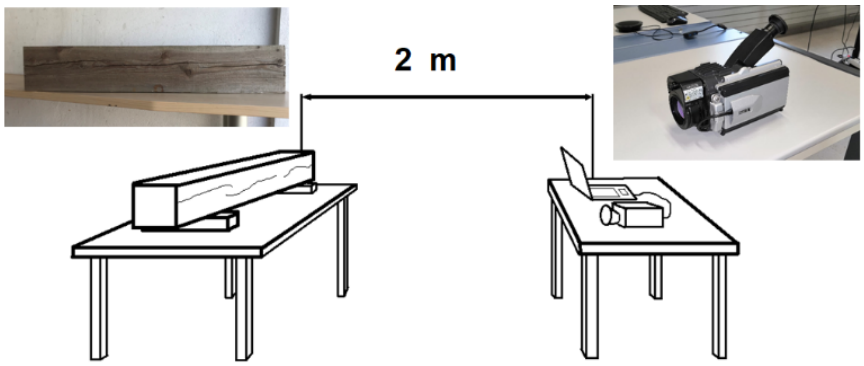

Fig.1: Experimental setup used in this work.

A Bosch EasyHeat 500 thermal pistol is used for the heating of the beams with a maximum power and maximum temperature of 1.6 kW and 500 °C, respectively. For the thermal measurements is used a NEC TH9260 thermographic camera, with 640 (horizontal) x 480 (vertical) pixels/temperature values for each thermal image acquired, resolution of 0.1 °C, accuracy of ±2 °C or ±2% of reading (whichever is greater), and spectral range from 8 to 14 µm. For the thermal image processing, the software of the thermographic camera, Image Processor Pro II ©, is used. Moreover, a 0.5 mm diameter wire is used for the manual depth measurements of each superficial crack. This wire is inserted into the crack, measuring the length penetrated.

In the first experiment (experiment 1), the thermal pistol is not used on the wooden beams, acquiring a single thermal image on each beam by the thermographic camera without previous thermal excitation on the beams. Meanwhile, in the second experiment (experiment 2), the surface of each beam is heated with the thermal pistol up to 90°C for 6 minutes. The temperature of 90 °C must not be exceeded, so that the properties of the beams are not affected, and the evaporation of the water contained in the beams is prevented. After the end of the heating, the thermographic camera starts recording the cooling process of the surfaces. A thermal image is taken every 2 seconds for 10 minutes. Then, a total of 300 thermal images is taken in each beam.

3. Methodology.

Two methodologies are proposed to meet the goal of analysing the geometric characteristics of superficial cracks in wooden beams using IRT as a technology:

1) The first method consists of analysing the surface temperature of each wooden beam measured by means of the experiment 1. In other words, the thermal behaviour of the beams at rest is studied. Specifically, the temperature value of each pixel from the thermal images is analysed to define the geometric characteristics of the cracks.

2) The second method consists of analysing the surface temperature of each wooden beam measured by means of the experiment 2. In other words, the thermal behaviour of the beams during their cooling is studied. Specifically, the temperature value of each pixel from the thermal images is analysed to define the geometric characteristics of the cracks.

Moreover, in order to check if the results obtained in both methodologies are adequate, the geometric properties of the cracks are also measured manually. Hence the use of the wire mentioned in the previous section.

4. Results and discussion.

In the first methodology, a total of 7 cracks are analysed, 3 for the pine beam (Beam 1) and 4 for the oak beam (Beam 2). As it can be seen in Figure 2, the cracks are clearly visible in the thermal images due to the existence of a thermal difference between these defects and the unaltered surroundings of the beams. Figure 3 shows a straight line crossing one of the cracks of Beam 1 on the thermal image acquired with the help of the Image Processor Pro II © (called 'Line – 1'), and a graph of how varies the temperature value along the pixels of the 'Line-1'.

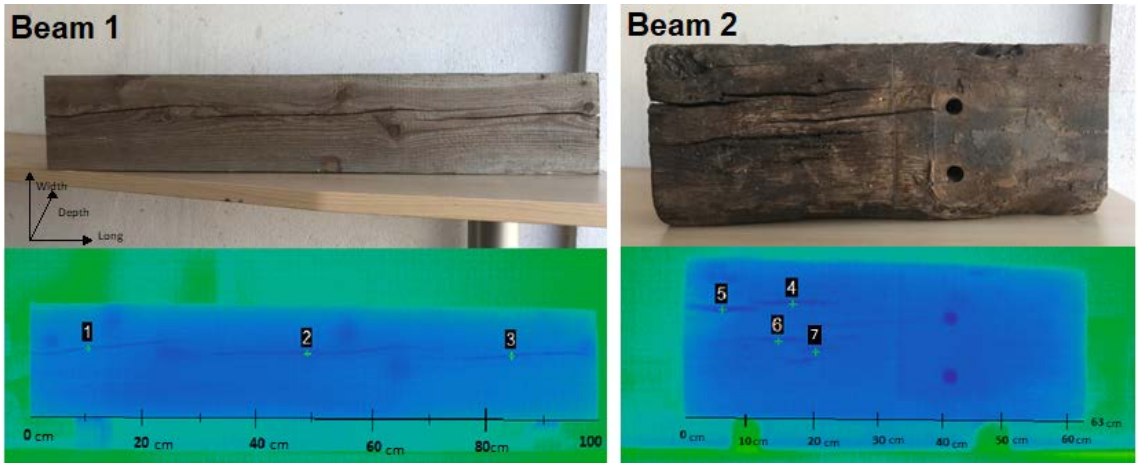

Fig. 2: Thermal image without previous thermal excitation of the Beam 1 and 2, indicating the 7 cracks to analyse.

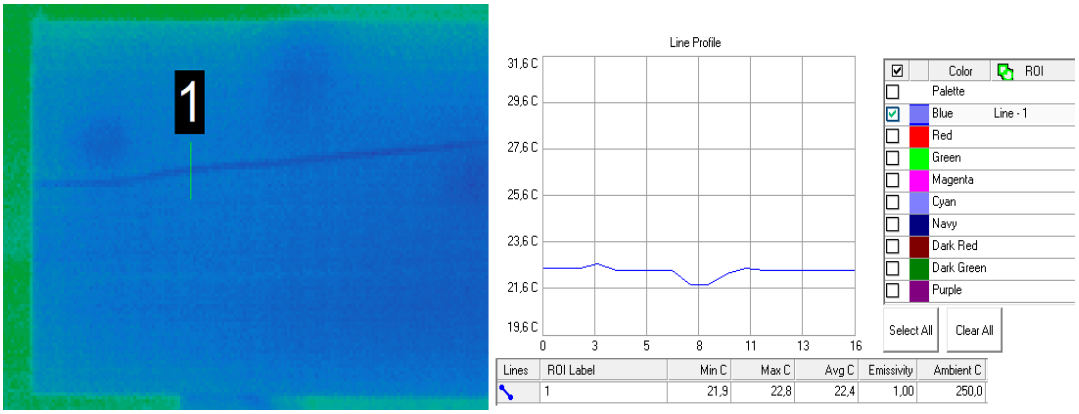

Fig. 3: Example of temperature variation (°C) crossing a crack (its width).

Table 1 compares the width measured in the thermal image with the real width measured manually for each crack (specifically cracks 1 and 2 (Beam 1), 6 and 7 (Beam 2)). This is done by counting the number of pixels of the straight line crossed in each crack on the thermal image and then multiplying by its equivalency ('distance/pixel' ratio) to estimate the width in metric units. The equivalency is obtained since the real width of each beam is previously known. In this case, the equivalency is 1.67 mm/pixel for both Beam 1 and Beam 2.

Table 1: Differences between manual measurements and using thermal images to obtain the width of the cracks.

Crack 1		Crack 2		Crack 6		Crack 7			
Width measured manually (cm)	Width thermal image (cm)	Width measured manually (cm)	Width thermal image (cm)	Width measured manually (cm)	Width thermal image (cm)	Width measured manually (cm)	Width thermal image (cm)		
0.2	0.154	0.21	0.173	0.52	0.709	1.1	1.25		
	Absolute error (cm)		Absolute error (cm)		Absolute error (cm)		Absolute error (cm)	Average absolute error (cm)	Average relative error (%)
	0.046		0.037		0.189		0.15	0.1055	20.8%

The average absolute/relative error obtained is 0.1055 cm/20.8%. This error could be reduced by using a thermographic camera with more resolution and more pixels in the thermal image. In the same way, Table 2 shows the long of each crack measured manually and compared with the width calculated using the thermal images (including all the cracks in this case). The average absolute/relative error obtained is 0.013 cm/0.05% in this case.

Table 2: Differences between manual measurements and using thermal images to obtain the long of the cracks.

Crack 1		Crack 2		Crack 3		Crack 4	
Long measured manually (cm)	Long thermal image (cm)	Long measured manually (cm)	Long thermal image (cm)	Long measured manually (cm)	Long thermal image (cm)	Long measured manually (cm)	Long thermal image (cm)
34	34.29	46	45.88	28	28.24	18	17.82
Crack 5		Crack 6		Crack 7			
Long measured manually (cm)	Long thermal image (cm)	Long measured manually (cm)	Long thermal image (cm)	Long measured manually (cm)	Long thermal image (cm)	Average absolute error (cm)	Average relative error (%)
14	13.95	30	30.25	20	19.66	0.013	0.05%

Moreover, Figure 4 illustrates the variation of depth in Crack 2 (Beam 1) versus the temperature value in each 2 cm section along the long of the Crack 2 (taking the lowest temperature in each section). In addition, in Figure 5 it is shown the width variation of Crack 2 versus the temperature value in the same sections used in Figure 4.

Figures 4 and 5 are modified by reversing the ordinate axis of the temperature. This is to clearly see the correlation between the increase of the depth/width/cross section of the crack and the decrease of temperature. Thus, as the depth/width/cross section of the crack increases, so does the temperature in the figures.

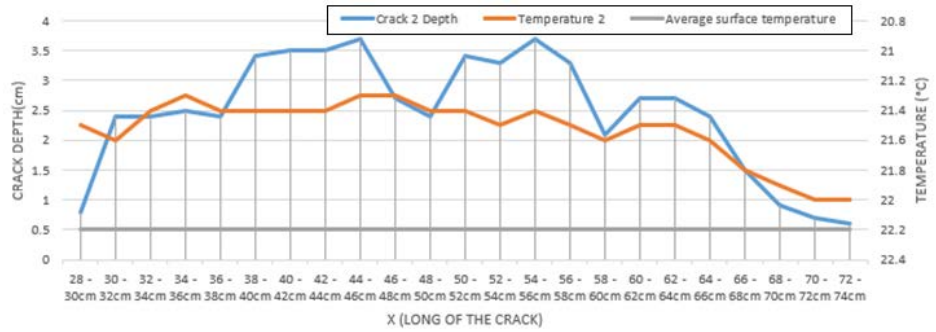

Fig. 4: Crack 2 of Beam 1: Variation of depth versus the temperature variation.

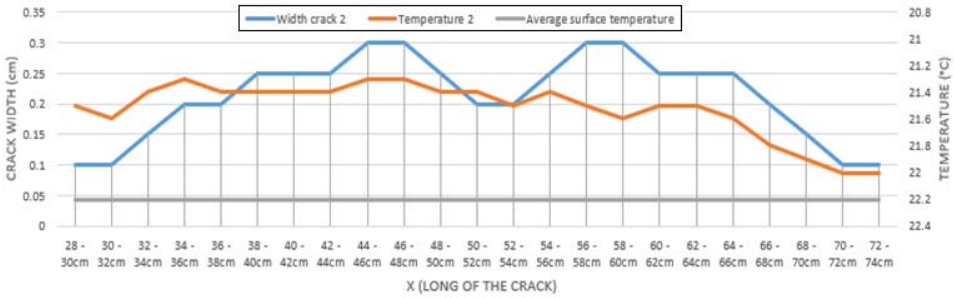

Fig. 5: Crack 2 of Beam 1: Variation of width versus the temperature variation.

Analysing the other cracks, there is an apparent relationship between temperature and depth in each crack. However, in Crack 6 and Crack 7 are found similar temperature values, but Crack 6 is a deep crack (maximum depth of 28mm) while Crack 7 is a shallow crack (maximum depth of 9mm). Then, this methodology 1 is not valid to analyse the crack depth (see Figure 6).

Therefore, it can be concluded that it is possible to measure the long and width of a crack and not its depth with the proposal of this first method. It should be noted that, in order to better understand the results, the average surface temperature at the time of the measurements is also shown from Figure 4 to Figure 6, where it can be seen that the average surface temperature of the beams is always lower than the temperature of the cracks.

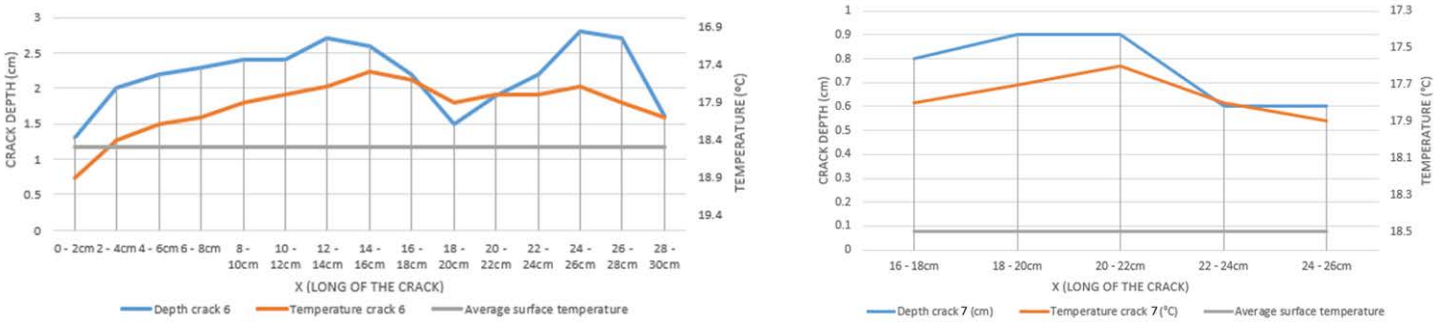

Fig. 6: a) Crack 6 of Beam 2: Depth variation versus temperature variation. b) Crack 7 of Beam 2: Depth variation versus temperature variation.

As for the second methodology, Figure 7.a presents a sequence of thermal images of the cooling process of Beam 1. In Figure 7.b, a 3D graph of the cooling process of Crack 2 of Beam 1 is shown.

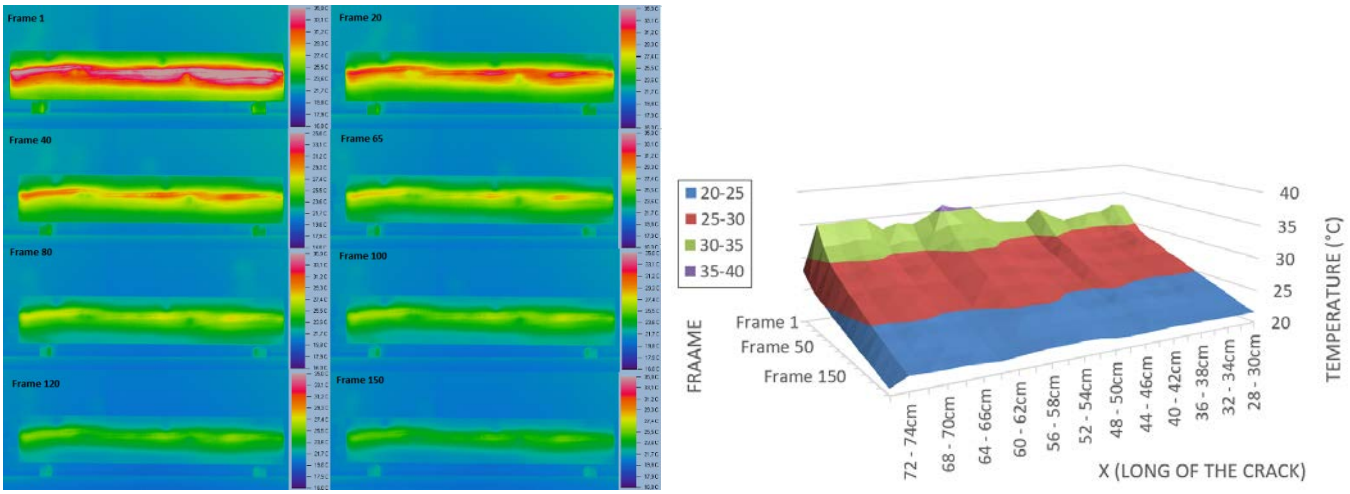

Fig. 7: a) Cooling of Beam 1. b) Crack 2 of Beam 1. Cooling in 3D.

As can be seen in Figure 7, during the first frames there is a high difference between the temperature in the cracks and the unaltered surroundings. From frame 80, the temperatures start to be similar and it is more complex to distinguish the presence of the cracks. The frames in which the cracks are more visible are from frame 20 to frame 40. In that time interval (frame 20 to frame 40), the surface of the beam stops dissipating heat except in the cracks, thus being the areas of the defects sharper. Similar thermal behaviour occurs in Beam 2 during the cooling process, with the interval of the frames in which the cracks are most clearly visible the same as in Beam 1.

The figures that show the relationship between temperature variation versus width/cross section variation during the cooling do not apport more useful data in comparison to the previous methodology. This is due to the way the surface is heated, with some areas with higher heat received than others inducing to an error. So, for the analysis of the crack long and width, it is more adequate to analyse the beams without previous thermal excitation (i.e., methodology 1).

However, analysing the cooling rate of the cracks, especially Crack 6 and Crack 7 (both of them belonging to Beam 2), it is possible to see how this cooling rate is related to the depth of the cracks. Then, it is possible to estimate the depth of the cracks with this second method, being more accurate than the first method. As a demonstration, Figures 8 and 9 show the cooling rate of Cracks 6 and 7, respectively, representing by the following 3 parameters defined for each crack:

a) Crack temperature in its deepest zone in every frame.

b) Maximum crack temperature in its surroundings in every frame.

c) Average temperature in the surface of the beam in every frame.

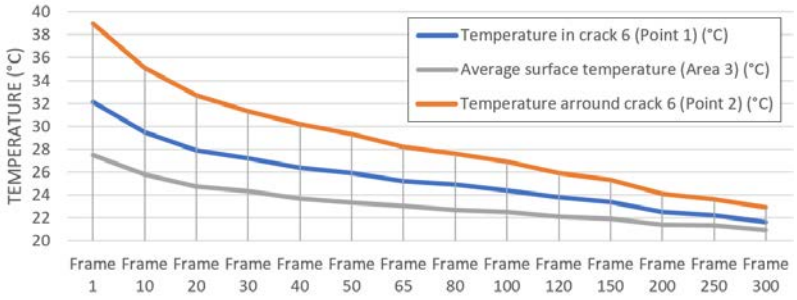

Fig. 8: Crack 6 of Beam 2: Cooling rate.

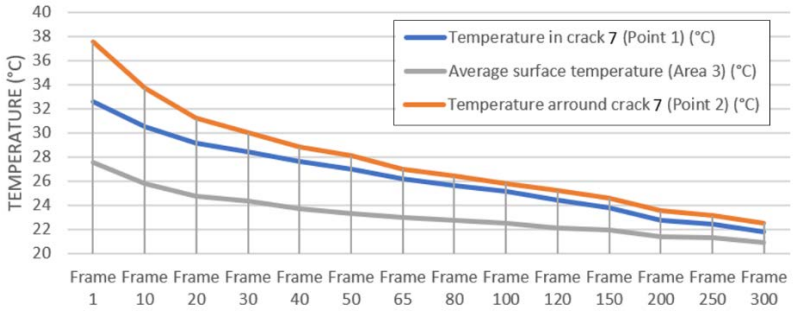

Fig. 9: Crack 7 of Beam 2: Cooling rate.

As it can be seen in Figures 8 and 9, the difference between maximum temperature around the crack and temperature inside the crack varies a lot between them. This leads to different cooling rates, and consequently different depths. Moreover, Figure 10 shows that the difference of temperatures between the hottest point and the coolest point in every frame in Crack 7 stabilizes before (frame 65) than Crack 6 (it is not possible to affirm if in frame 300 is already stabilized). Therefore, based on these results, it can be determined if a crack is deep by the time it takes to stabilize its temperature.

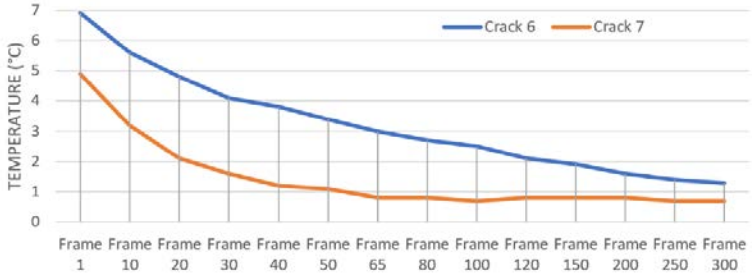

Fig. 10: Temperature difference between the hottest point and the coolest point of the Cracks 6 and 7 during the cooling.

4. Conclusion

Based on the results that were obtained after the application of the methodologies proposed in this work, it can be concluded that the long and width of the cracks can be measured using the thermal images of the wooden beams without previous thermal excitation (methodology 1). However, it is observed how low depth cracks have temperature gradient similar to high depth cracks in these images without previous thermal excitation. Then, methodology 1 is not a good method to estimate depth. As for methodology 2, focusing on the sequence of thermal images in each wooden beam acquired during their cooling after a previous heating, and specifically in the cooling rate of the cracks that have low depth compared to the ones with high depth, it can be observed that the cooling rate of low depth cracks is higher. With this, it is concluded that by a previous heating, an estimation of the depth can be made with the thermal images acquired during the cooling.

Therefore, a combination of the two methods proposed in this work can be satisfactorily used to determine the geometric characteristics of a crack in a wooden beam. Future projects should focus on automating the methodologies proposed by developing algorithms that automatically relate the width and long of the cracks to their number of pixels, and the depth of the cracks to their cooling rates.

Acknowledgements

This work has been partially supported by the Spanish Ministry of Science, Innovation and Universities through the project Ref. RTI2018-095893-B-C21, and the SIRMA project, which is co-financed by the INTERREG Atlantic Area Programme through the European Regional Development Fund (ERDF) with application code: EAPA_826/2018.

References

[1] M. Cabaleiro, R. Lindenbergh, W.F. Gard, P. Arias, J.W.G van de Kuilen, Algorithm for automatic detection and analysis of cracks in timber beams from LiDAR data. Construction and Building Materials, 130, 41-53. (2017)

[2] J. Cuartero, M.Cabaleiro, H.S. Sousa, J.M. Branco, Tridimensional parametric model for prediction of structural safety of existing timber roofs using laser scanner and drilling resistance tests, Engineering Structures, 185 (2019) 58-67.

[3] M. Cabaleiro, J.M. Branco, H.S Sousa, B. Conde, First results on the combination of laser scanner and drilling resistance tests for the assessment of the geometrical condition of irregular cross-sections of timber beams, Materials and Structures, 51(4) (2018) 99.

[4] A. Mol, M. Cabaleiro, H.S. Sousa, J.M. Branco, HBIM for storing life-cycle data regarding decay and damage in existing timber structures. *Automation in Construction*, *117* (2020) 103262.

[5] Luis Sánchez Calderón, Jesus Bairán, Crack Detection in Concrete Elements from RGB Pictures using Modified Line Detection Kernels (2017)

[6] Iván Garrido, Susana Lagüela y Pedro Arias, Infrared Thermography's Application to Infrastructure Inspections (2018).

[7] Carosena Meola, A new approach for estimation of defects detection with infrared thermography, Materials Letters 61 (2007) 747–750.

[8] Fabio Bisegna, Dario Ambrosini, Domenica Paoletti, Stefano Sfarra, Franco Gugliermetti, A qualitative method for combining thermal imprints to emerging weak points of ancient wall structures by passive infrared thermography – A case study, Journal of Cultural Heritage 15 (2014) 199–202.

[9] Gokhan Kilic, Using advanced NDT for historic buildings: Towards an integrated multidisciplinary health assessment strategy, Journal of Cultural Heritage 16 (2015) 526–535.

[10] Ali Foudazi, Ali Mirala, Mohammad Tayeb Ghasr and Kristen M. Donnell, Active Microwave Thermography for Nondestructive Evaluation of Surface Cracks in Metal Structures, IEEE TRANSACTIONS ON INSTRUMENTATION AND MEASUREMENT, VOL. 68, NO. 2, FEBRUARY 2019.

[11] Tobias Pahlberg, Matthew Thurley, Djordje Popovic, Olle Hagman, Crack detection oak flooring lamellae using ultrasound-excited thermography, Infrared Physics & Technology 88 (2018) 57–69.

[12] Gamaliel López, Luis-Alfonso Basterra, Luis Acuña, Infrared thermography for wood density estimation, Infrared Physics & Technology 89 (2018) 242–246.

[13] A. Wyckhuyse, X. Maldague, A Study of Wood Inspection by Infrared Thermography, Part I: Wood Pole Inspection by Infrared Thermography, Electrical and Computing Engineering Department, Université Laval, Quebec City, Quebec, Canada (2001).

[14] D. Wu, G. Busse, Remote inspection of wood with lock-in-thermography, in: TAPPI 1995 European Plastic Laminates Symposium, vol. 79, no. 8, 1995, pp. 119–123.

[15] J. Sembach, D.S.A.H.G. Wu, G. Busse, Non-destructive evaluation of delaminations in laminated wood-based panels by thermographical inspection tools, in: Proc. of Workshop on Nondestructive Testing of Panel Products, 11 October, Llandudno, UK, J. Hague, 1997, pp. 41-48.

[16] G. López, L.A. Basterra, G. Ramón-Cueto, A. de Diego, Detection of singularities and subsurface defects in wood by infrared thermography, Int. J. Archit. Heritage 8 (2014) 517–536.

[17] M. Solla, S.Lagüela, H.González-Jorge, P.Arias, Approach to identify cracking in asphalt pavement using GPR and infrared thermographic methods: Preliminary findings, NDT&E International62 (2014)55–65.